Supporting Information for

Characteristic Features of CO_2 and CO Adsorptions to Paddle-Wheel-type Porous Coordination Polymer

Jia-Jia Zheng,[†,‡] Shinpei Kusaka,[†] Ryotaro Matsuda,[†,§] Susumu Kitagawa,[*,†,ǁ] and Shigeyoshi Sakaki[*,‡]

[†]Institute for Integrated Cell-Material Sciences (WPI-iCeMS), Kyoto University, Ushinomiya cho, Yoshida, Sakyo-ku, Kyoto, 606-8501, Japan

[‡]Fukui Institute for Fundamental Chemistry, Kyoto University, Nishi-hiraki cho, Takano, Sakyo-ku, Kyoto 606-8103, Japan

[§] Department of Chemistry and Biotechnology, School of Engineering, Nagoya University, Chikusa-ku, Nagoya 464-8603, Japan

[ǁ]Department of Synthetic Chemistry and Biological Chemistry, Graduate School of Engineering, Kyoto University, Katsura, Nishikyo-ku, Kyoto 615-8510, Japan

*E-mail: kitagawa@icems.kyoto-u.ac.jp; sakaki.shigeyoshi.47e@st.kyoto-u.ac.jp

Table of Contents

List of complete authors for ref. 54, 62, and 64

(54) Chung, L. W.; Sameera, W. M. C.; Ramozzi, R.; Page, A. J.; Hatanaka, M.; Petrova, G. P.; Harris, T. V.; Li, X.; Ke, Z.; Liu, F.; Li, H.-B.; Ding, L.; Morokuma, K. The ONIOM Method and Its Applications. *Chem. Rev.* **2015**, *115*, 5678-5796.

(62) Frisch, M. J.; Trucks, G. W.; Schlegel, H. B.; Scuseria, G. E.; Robb, M. A.; Cheeseman, J. R.; Scalmani, G.; Barone, V.; Mennucci, B.; Petersson, G. A.; Nakatsuji, H.; Caricato, M.; Li, X.; Hratchian, H. P.; Izmaylov, A. F.; Bloino, J.; Zheng, G.; Sonnenberg, J. L.; Hada, M.; Ehara, M.; Toyota, K.; Fukuda, R.; Hasegawa, J.; Ishida, M.; Nakajima, T.; Honda, Y.; Kitao, O.; Nakai, H.; Vreven, T.; Montgomery, Jr., J. A.; , Peralta, J. E.; Ogliaro, F.; Bearpark, M.; Heyd, J. J.; Brothers, E.; Kudin, K. N.; Staroverov, V. N.; Keith, T.; Kobayashi, R.; Normand, J.; Raghavachari, K.; Rendell, A.; Burant, J. C.; Iyengar, S. S.; Tomasi, J.; Cossi, M.; Rega, N.; Millam, J. M.; Klene, M.; Knox, J. E.; Cross, J. B.; Bakken, V.; Adamo, C.; Jaramillo, J.; Gomperts, R.; Stratmann, R. E.; Yazyev, O.; Austin, A. J.; Cammi, R.; Pomelli, C.; Ochterski, J. W.; Martin, R. L.; Morokuma, K.; Zakrzewski, V. G.; Voth, G. A.; Salvador, P.; Dannenberg, J. J.; Dapprich, S.; Daniels, A. D.; Farkas, O.; Foresman, J. B.; Ortiz, J. V.; Cioslowski, J.; Fox, D. J. *Gaussian 09*, revision D.01; Gaussian, Inc: Wallingford, CT, 2013.

(64) Schmidt, M. W.; Baldridge, K. K.; Boatz, J. A.; Elbert, S. T.; Gordon, M. S.; Jensen, J. H.; Koseki, S.; Matsunaga, N.; Nguyen, K. A.; Su, S.; Windus, T. L.; Dupius, M.; Montgomery Jr, J. A. General Atomic and Molecular Electronic Structure System. *J. Comput. Chem.* **1993**, *14*, 1347-1363.

Evaluation of binding energy by the ONIOM procedure

The binding energy of L with Mm-R is represented by eq.1 in the ONIOM scheme;

$$\mathrm{BE}^{\mathrm{Mm}} = \mathrm{BE}^{\mathrm{Low}}_{\mathrm{Mm\text{-}R}} + \mathrm{BE}^{\mathrm{High}}_{\mathrm{SM1}} - \mathrm{BE}^{\mathrm{Low}}_{\mathrm{SM1}} \quad (1)$$

where the superscripts "Low" and "High" represent the low-level and high-level calculations, respectively. Similarly, the binding energy of L at the α site with Dm-R can be calculated by eq.2;

$$\mathrm{BE}^{\alpha} = \mathrm{BE}^{\alpha\mathrm{Low}}_{\mathrm{Dm\text{-}R}} + \mathrm{BE}^{\alpha\mathrm{High}}_{\mathrm{SM1}} - \mathrm{BE}^{\alpha\mathrm{Low}}_{\mathrm{SM1}} \quad (2)$$

In evaluating the binding energy BE^{β} at the β site, we need to consider two small models SM1 and SM2 at the high level (eq. 3), because the L interacts with the Cu center and two phenyl moieties of the neighbor paddle-wheel unit;

$$\mathrm{BE}^{\beta} = \mathrm{BE}^{\beta\mathrm{Low}}_{\mathrm{Dm\text{-}R}} + (\mathrm{BE}^{\beta\mathrm{High}}_{\mathrm{SM1}} - \mathrm{BE}^{\beta\mathrm{Low}}_{\mathrm{SM1}}) + (\mathrm{BE}^{\beta\mathrm{High}}_{\mathrm{SM2}} - \mathrm{BE}^{\beta\mathrm{Low}}_{\mathrm{SM2}}) \quad (3)$$

The $\mathrm{BE}^{\mathrm{Low}}_{\mathrm{Mm\text{-}R}}$, $\mathrm{BE}^{\alpha\mathrm{Low}}_{\mathrm{Dm\text{-}R}}$, and $\mathrm{BE}^{\beta\mathrm{Low}}_{\mathrm{Dm\text{-}R}}$ are calculated with eqs. 4-6.

$$\mathrm{BE}^{\mathrm{Low}}_{\mathrm{Mm\text{-}R}} = E^{\mathrm{Low}}_{\mathrm{Mm\text{-}R\text{-}2L}} / 2 - E^{\mathrm{Low}}_{\mathrm{Mm\text{-}R}} / 2 - E^{\mathrm{Low}}_{\mathrm{L}} \quad (4)$$

$$\mathrm{BE}^{\alpha\mathrm{Low}}_{\mathrm{Dm\text{-}R}} = E^{\mathrm{Low}}_{\mathrm{Dm\text{-}R\text{-}4L}} / 2 - E^{\mathrm{Low}}_{\mathrm{Dm\text{-}R\text{-}2L^{\beta}}} / 2 - E^{\mathrm{Low}}_{\mathrm{L}} \quad (5)$$

$$\mathrm{BE}^{\beta\mathrm{Low}}_{\mathrm{Dm\text{-}R}} = E^{\mathrm{Low}}_{\mathrm{Dm\text{-}R\text{-}4L}} / 2 - E^{\mathrm{Low}}_{\mathrm{Dm\text{-}R\text{-}2L^{\alpha}}} / 2 - E^{\mathrm{Low}}_{\mathrm{L}} \quad (6)$$

where $E^{\mathrm{Low}}_{\mathrm{Mm\text{-}R\text{-}2L}}$ and $E^{\mathrm{Low}}_{\mathrm{Mm\text{-}R}}$ are the total energies of monomer models with and without L, and $E^{\mathrm{Low}}_{\mathrm{L}}$ is the total energy of one gas molecule, $E^{\mathrm{Low}}_{\mathrm{Dm\text{-}R\text{-}4L}}$ is total energy of dimer model with 4 gas molecules, and $E^{\mathrm{Low}}_{\mathrm{Dm\text{-}R\text{-}2L^{\alpha}}}$ and $E^{\mathrm{Low}}_{\mathrm{Dm\text{-}R\text{-}2L^{\beta}}}$ are total energies of dimer model with 2 gas molecules at the α and β positions, respectively.

The $\mathrm{BE}^{\mathrm{High}}_{\mathrm{SM1}}$, $\mathrm{BE}^{\alpha\mathrm{High}}_{\mathrm{SM1}}$, $\mathrm{BE}^{\beta\mathrm{High}}_{\mathrm{SM1}}$ and $\mathrm{BE}^{\beta\mathrm{High}}_{\mathrm{SM2}}$ are calculated with eqs. 7-10.

$$\mathrm{BE}^{\mathrm{High}}_{\mathrm{SM1}} = E^{\mathrm{High}}_{\mathrm{SM1\text{-}2L}} / 2 - E^{\mathrm{High}}_{\mathrm{SM1}} / 2 - E^{\mathrm{High}}_{\mathrm{L}} \quad (7)$$

$$\mathrm{BE}^{\alpha\mathrm{High}}_{\mathrm{SM1}} = E^{\mathrm{High}}_{\mathrm{SM1\text{-}2L}} - E^{\mathrm{High}}_{\mathrm{SM1\text{-}L^{\beta}}} - E^{\mathrm{High}}_{\mathrm{L}} \quad (8)$$

$$\mathrm{BE}^{\beta\mathrm{High}}_{\mathrm{SM1}} = E^{\mathrm{High}}_{\mathrm{SM1\text{-}2L}} - E^{\mathrm{High}}_{\mathrm{SM1\text{-}L^{\alpha}}} - E^{\mathrm{High}}_{\mathrm{L}} \quad (9)$$

$$\mathrm{BE}^{\beta\mathrm{High}}_{\mathrm{SM2}} = E^{\mathrm{High}}_{\mathrm{SM2\text{-}L}} - E^{\mathrm{High}}_{\mathrm{SM2}} - E^{\mathrm{High}}_{\mathrm{SM2}} \quad (10)$$

where $E^{\mathrm{High}}_{\mathrm{SM1\text{-}2L}}$, $E^{\mathrm{High}}_{\mathrm{SM1}}$, $E^{\mathrm{High}}_{\mathrm{SM2\text{-}L}}$, $E^{\mathrm{High}}_{\mathrm{SM2}}$ and $E^{\mathrm{High}}_{\mathrm{L}}$ are total energies of SM1 with two L, SM1, SM2 with one L, SM2 and L, and $E^{\mathrm{High}}_{\mathrm{SM1\text{-}L^{\alpha}}}$ and $E^{\mathrm{High}}_{\mathrm{SM1\text{-}L^{\beta}}}$ are total energies of SM1 with one gas

molecule at the α and β positions, respectively. The BE_{SM1}^{Low}, $BE_{SM1}^{\alpha Low}$, $BE_{SM1}^{\beta Low}$ and $BE_{SM2}^{\beta Low}$ are calculated in similar ways to eqs. 7-10 at the low level.

Table S1. Geometrical parameters of monomer model Mm-R with adsorbed gas molecules.

	Mm-H					Mm-Me				
	Non	CO	N_2	NO	CO_2	None	CO	N_2	NO	CO_2
Cu-Cu/Å	2.507	2.586	2.547	2.541	2.540	2.505	2.584	2.543	2.538	2.538
Cu-O/Å	1.965	1.981	1.973	1.973	1.973	1.963	1.978	1.972	1.972	1.973
Cu-A^1/Å [a]	-	2.409	2.468	2.473	2.420	-	2.410	2.474	2.477	2.428
Cu-Cu-X^1/°	-	180	180	175	167	-	180	180	175	167
Cu-X^1-X^2/°	-	180	180	122	117	-	180	180	122	117
O^C-Cu-X^1-X^2/° [b]	-	-	-	0	3		-	-	0	3

[a] X^1 and X^2 represent atoms in gas molecules; CO: X^1 = C, X^2 = O; N_2: X^1 = N, X^2=N; NO: X^1 = N, X^2 = O; CO_2: X^1 = O, X^2 = C.

[b] O^C represents one O atom of carboxylate groups in a paddle-wheel unit.

Table S2. NBO charges (*e*) for atoms and atomic groups in Mm-R (R = H, and Me).

	Mm-H				Mm-Me			
	CO	N_2	NO	CO_2	CO	N_2	NO	CO_2
Cu	0.926	1.018	1.001	1.061	0.925	1.017	1.002	1.062
O	–0.712	–0.714	–0.713	–0.720	–0.712	–0.714	–0.713	–0.718
C_6H_4-R	0.008	0.011	0.011	0.013	0.008	0.011	0.011	0.013
O_2C-C_6H_4-R	–0.552	–0.554	–0.551	–0.557	–0.551	–0.553	–0.551	–0.557
L	0.178	0.089	0.101	0.053	0.177	0.088	0.101	0.053

Table S3. Geometrical parameters of dimer model Dm-R with adsorbed gas molecules.

	Dm-H					Dm-Me				
	Non	CO	N_2	NO	CO_2	Non	CO	N_2	NO	CO_2
(A)	4L									
Cu^{α}-Cu^{β}/Å	2.548	2.626 (2.580) [d]	2.587	2.592	2.609	2.528	2.607 (2.580) [d]	2.566	2.571	2.587
Cu^{β}-Cu^{β}/Å	4.819	4.628 (4.642)	4.744	4.818	4.706	4.952	4.807 (4.642)	4.895	4.939	4.836
<Cu-O>/Å [a]	1.964	1.982 (1.910)	1.974	1.974	1.977	1.964	1.981 (1.910)	1.973	1.975	1.976
Cu^{α}-$X^{1\alpha}$/Å [b]	-	2.394	2.443	2.454	2.453	-	2.409	2.452	2.471	2.471
Cu^{β}-$X^{1\beta}$/Å	-	2.388	2.498	2.508	2.398	-	2.382	2.453	2.468	2.382
Cu^{β}-Cu^{α}-$X^{1\alpha}$/°	-	179	179	175	158	-	180	180	174	160
Cu^{α}-$X1^{\alpha}$-$X^{2\alpha}$/°	-	180	178	120	109	-	179	178	122	109
Cu^{α}-Cu^{β}-$X^{1\beta}$/°	-	169	167	171	169	-	175	175	175	171
Cu^{β}-$X^{1\beta}$-$X^{2\beta}$/°	-	170	165	120	119	-	173	170	122	118
$O^{C\alpha}$-Cu^{α}-$X^{1\alpha}$-$X^{2\alpha}$/° [c]	-	45	45	6	40	-	45	45	1	38
$O^{C\beta}$-Cu^{β}-$X^{1\beta}$-$X^{2\beta}$/°	-	45	45	42	13	-	45	45	42	11
(B)	$2L^{\alpha}$									
Cu^{α}-Cu^{β}/Å	2.548	2.587	2.567	2.567	2.580	2.528	2.568	2.544	2.540	2.585
Cu^{β}-Cu^{β}/Å	4.819	4.652	4.680	4.734	4.653	4.952	4.775	4.877	4.899	4.784
<Cu-O>/Å	1.964	1.974	1.970	1.971	1.972	1.964	1.973	1.969	1.970	1.973
Cu^{α}-$X^{1\alpha}$/Å	-	2.374	2.436	2.442	2.410	-	2.387	2.445	2.452	2.424
Cu^{β}-Cu^{α}-$X^{1\alpha}$/°	-	179	179	174	160	-	179	179	175	159
Cu^{α}-$X^{1\alpha}$-$X^{2\alpha}$/°	-	180	179	123	113	-	180	178	122	111
$O^{C\alpha}$-Cu^{α}-$X^{1\alpha}$-$X^{2\alpha}$/°	-	45	45	5	10	-	45	45	1	37
(C)	$2L^{\beta}$									
Cu^{α}-Cu^{β}/Å	2.548	2.594	2.570	2.581	2.589	2.528	2.576	2.550	2.562	2.568
Cu^{β}-Cu^{β}/Å	4.819	4.837	4.862	4.862	4.790	4.952	4.937	4.973	4.955	4.925
<Cu-O>/Å	1.964	1.974	1.963	1.718	1.971	1.964	1.974	1.969	1.969	1.971
Cu^{β}-$X^{1\beta}$/Å	-	2.378	2.473	2.491	2.379	-	2.370	2.445	2.464	2.370
Cu^{α}-Cu^{β}-$X^{1\beta}$/°	-	171	169	172	170	-	176	175	176	172
Cu^{β}-$A^{1\beta}$-$X^{2\beta}$/°	-	171	167	121	120	-	174	172	122	119
$O^{C\beta}$-Cu^{β}-$X^{1\beta}$-$X^{2\beta}$/°	-	45	45	45	13	-	45	45	45	9

[a] Average value of eight Cu-O bonds in one Cu paddle-wheel unit.
[b] X^1 and X^2 represent atoms in gas molecules; CO: X^1 = C, X^2 = O; N_2: X^1 = N, X^2=N; NO: X^1 = N, X^2 = O; CO_2: X^1 = O, X^2 = C.
[c] O^C represents one O atom of carboxylate groups in a paddle-wheel unit.
[d] In parentheses are experimental results of CO-adsorbed Cu(aip)-PCP.[1]

Discussion of the change in geometrical parameters by adsorption of gas molecule:

The Cu^{α}-Cu^{β}, Cu^{β}-Cu^{β}, the averaged Cu-O distances of Dm-H-CO agree with the experimental values, as shown in Table S3 (column A); the averaged Cu-O(carboxylate) distance is moderately longer than the experimental value but the difference is not large. However, the calculated Cu^{β}-Cu^{β} distance is somewhat longer than the experimental value in the case of Dm-Me-CO, while the Cu^{α}-Cu^{β} distance agrees with the experimental value. This longer Cu^{β}-Cu^{β} distance would arise from the steric repulsion of the methyl group with the carboxylate of the next $[Cu_2(O_2C\text{-}C_6H_4\text{-}Me)_4]$ unit (denoted **B** in Scheme S1(A)); the steric repulsion enlarges the intermolecular distance between two $[Cu_2(O_2C\text{-}C_6H_4\text{-}Me)_4]$ units (**A** and **B**). In the real infinite system, however, such increase in the intermolecular distance would not occur, as shown in Scheme S1(B), because one more $[Cu_2(O_2C\text{-}C_6H_4\text{-}Me)_4]$ unit (denoted **C** in Scheme S1(B)) pushes back the central $[Cu_2(O_2C\text{-}C_6H_4\text{-}Me)_4]$ unit (**A** in Scheme S1(B)). These results suggest that the optimized Cu^{α}-Cu^{β}, Cu^{β}-Cu^{β}, and the average Cu-O distances agree with the experimental values in the cluster model, in which the steric repulsion is not large. We wish to focus on the geometry changes in Dm-H hereafter because the steric repulsion is small between the two dimer units.

It is interesting to investigate how the Cu^{α}-Cu^{β}, Cu^{β}-Cu^{β}, and the average Cu-O distances change by the adsorption of gas molecule. When all Cu^{α} and Cu^{β} sites interact with gas molecule (Table S3 column A), the Cu^{α}-Cu^{β} distance becomes longer, the Cu^{β}-Cu^{β} becomes shorter, and the averaged Cu-O distance becomes moderately longer except for the NO adsorption system in which the geometrical changes are small, as shown in Table S3(A). The elongation of the Cu^{α}-Cu^{β} distance occurs by the interaction of gas molecule because the gas molecule interacts with the Cu 4p orbital to decrease the 4p-4p bonding interaction between the Cu^{α} and Cu^{β} atoms and also raises the Cu $3d_{z2}$ orbital energy to enhance the d_{z2}-d_{z2} repulsion between the Cu^{α} and Cu^{β} atoms. As a result, the Cu^{α}-Cu^{β} elongation occurs by the gas adsorption, which further decreases the Cu^{β}-Cu^{β} distance.

When gas molecule interacts only with the Cu^{α} site (Table S3 column B), the Cu^{α}-Cu^{β} distance increases to a lesser extent than that induced by interactions of four gas molecules with all Cu^{α} and Cu^{β} sites. However, the change in the Cu^{β}-Cu^{β} distance is not simple; it decreases to a less extent than that by interaction of four molecules with all Cu sites in the CO adsorption and it more decreases in the N_2, NO, and CO_2 adsorption systems. When gas molecule interacts only with the Cu^{β} site (Table S3 column C), the Cu^{α}-Cu^{β} distance increases to a lesser extent than that induced by interaction of four molecules with all Cu^{α} and Cu^{β} sites. The Cu^{β}-Cu^{β} distance moderately increases unexpectedly because gas molecule between two Cu^{β} atoms induces the steric repulsion with another $[Cu_2(O_2C\text{-}C_6H_4\text{-}Me)_4]$ unit to increase the intermolecular distance between two $[Cu_2(O_2C\text{-}C_6H_4\text{-}Me)_4]$ units.

It is likely concluded that the interaction of gas molecule with both Cu^{α} and Cu^{β} atoms are important for discussing the geometry changes by gas interaction.

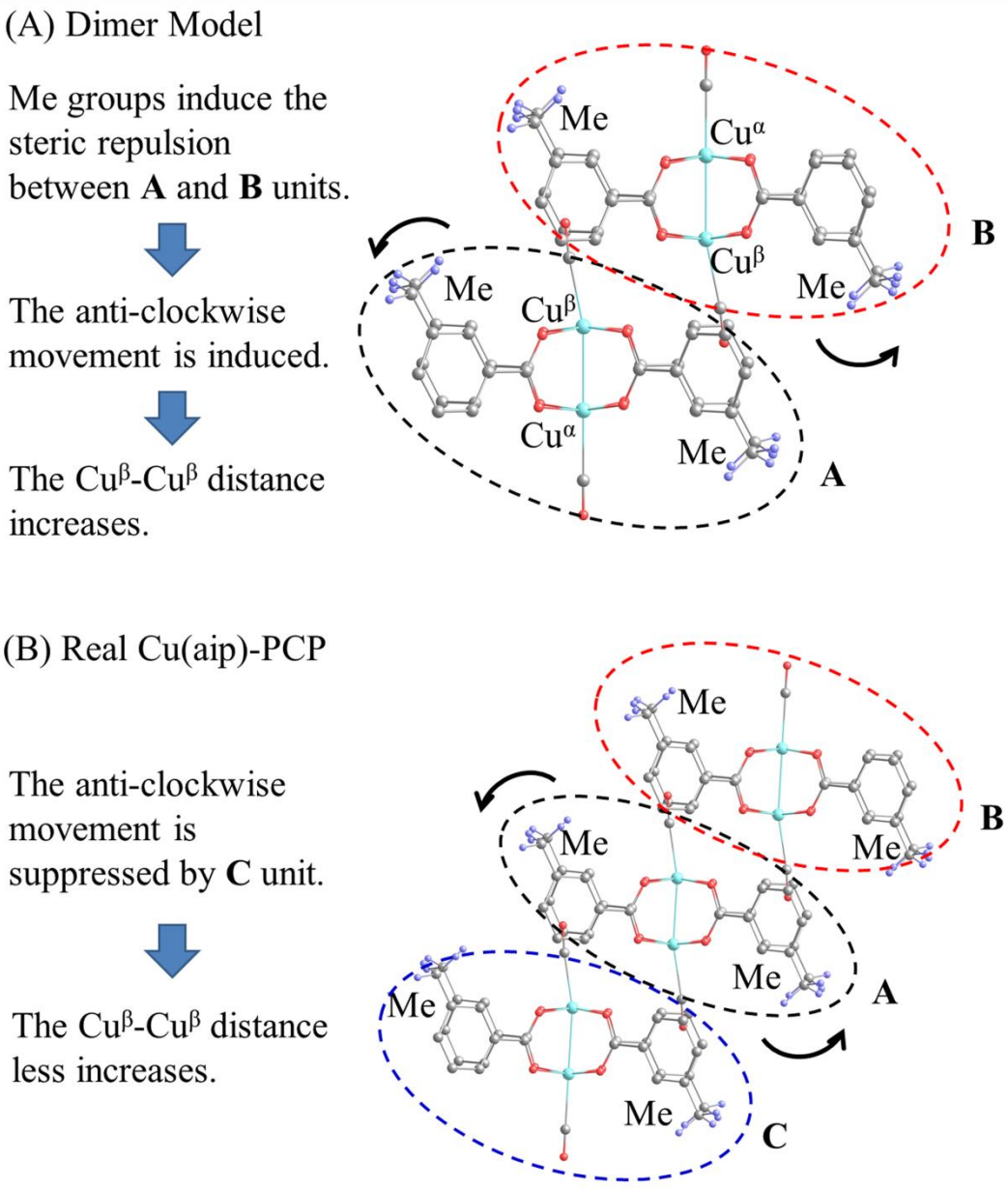

Scheme S1. Schematic representation of (A) Dm-Me and (B) real Cu(aip)-PCP.

Table S4. NBO charges (*e*) for Dm-R (R = H, and Me).

	Dm-H				Dm-Me			
	CO	N_2	NO	CO_2	CO	N_2	NO	CO_2
Cu^{α}	0.934	1.022	1.022	1.090	0.929	1.014	1.003	1.083
Cu^{β}	0.987	1.085	1.090	1.141	0.986	1.080	1.093	1.149
O^{α} [a]	–0.711	–0.713	–0.712	–0.723	–0.709	–0.711	–0.713	–0.723
O^{β} [a]	–0.732	–0.740	–0.743	–0.743	–0.736	–0.741	–0.746	–0.747
C_6H_4-R [b]	0.016	0.019	0.023	0.015	0.019	0.021	0.016	0.017
O_2C-C_6H_4-R	–0.570	–0.576	–0.574	–0.584	–0.570	–0.574	–0.577	–0.585
L^{α}	0.182	0.094	0.080	0.049	0.179	0.094	0.103	0.048
L^{β}	0.179	0.103	0.104	0.058	0.185	0.110	0.111	0.058

[a] O^{α} and O^{β} represent the average NBO charges of four oxygen atoms coordinated to Cu^{α} and Cu^{β}, respectively.

[b] Phenyl moieties (C_6H_4R, R = H and Me) in Dm-R neighboring to the adsorbed L^{β} molecules.

Table S5. Various interaction terms (kcal mol^{-1}) of gas molecule with the SM1 and SM2.[a]

	SM1						SM2					
L	BE^{HF}_{SM1}	ES	EXR	CT+Pol+Mix	DIS	$BE^{MP4(SDQ)}_{SM1}$	BE^{HF}_{SM2}	ES	EXR	CT+Pol+Mix	DIS	$BE^{MP4(SDQ)}_{SM2}$
CO^{N}	–3.43	–15.01	18.49	–6.82	–3.61	–7.04	4.97	–4.55	10.50	–0.98	–4.22	0.75
CO^{β}	–3.27	–15.07	18.63	–6.84	–3.64	–6.91	2.84	–2.41	5.85	–0.60	–3.53	–0.69
N_2^{N}	–1.17	–6.48	8.61	–3.30	–2.63	–3.80	5.98	–3.16	9.84	–0.70	–4.79	1.19
N_2^{β}	–1.01	–6.44	8.75	–3.32	–2.67	–3.68	2.95	–1.64	4.91	–0.32	–3.46	–0.51
NO^{N}	–0.05	–4.54	7.90	–3.43	–4.00	–4.05	6.21	–3.29	10.70	–1.20	–4.28	1.93
NO^{β}	–0.02	–4.98	9.16	–4.20	–4.00	–3.98	2.12	–1.82	5.64	–1.70	–3.07	–0.95
CO_2^{N}	–3.58	–12.27	13.06	–4.37	–1.74	–5.32	2.06	–3.43	6.46	–0.97	–3.34	–1.28
CO_2^{β}	–3.90	–11.37	11.64	–4.16	–1.29	–5.19	1.60	–3.06	5.45	–0.80	–3.26	–1.66

[a] R = Me. The binding energy was analyzed at both the normal position (L^{N}) and deviating position (L^{β}).

Table S6. CO binding energies (kcal mol^{-1}) at the β site of two Cu paddle-wheel units $[Cu_2(O_2CC_6H_4\text{-}R)_4]_2$ (H, CH_3, CF_3, OCH_3, and ^{t}Bu).

R [a]	DIS [b]	$BE^{MP4(SDQ)}_{SM2}$ [c]	BE^{β} [d]
CF_3	–3.91	0.10	–7.19
CH_3	–3.97	–0.20	–7.28
OCH_3	–4.25	–0.45	–7.26
^{t}Bu	–4.40	–0.54	–7.47

[a] Note that the comparison with R = H is not presented here because the introduction of these substituents induces the orientation change of phenyl moiety of the linker and such geometry change influences the binding energy; in other words, simple comparison with Dm-H is difficult.

[b,c] MP4(SDQ)-calculated dispersion interaction (DIS) and binding energy ($BE^{SM2}_{MP4(SDQ)}$) between CO and SM2. In these calculations, SM2 was constructed by replacing one meta-H in $PhCOO^-$ with various R substituents, keeping the other parts and CO position to be the same as those in the optimized $[Cu_2(O_2CC_6H_4\text{-}H)_4]_2$.

[d] The ONIOM[MP4(SDQ):ωB97XD]-calculated binding energy.

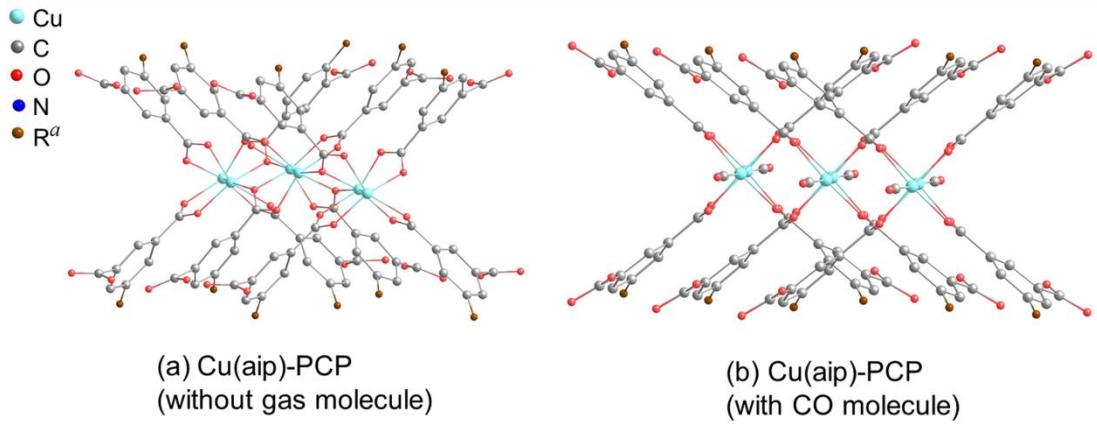

Figure S1. Another side view of structures of Cu(aip)-PCP (a) without gas molecule and (b) with adsorbed CO molecules.

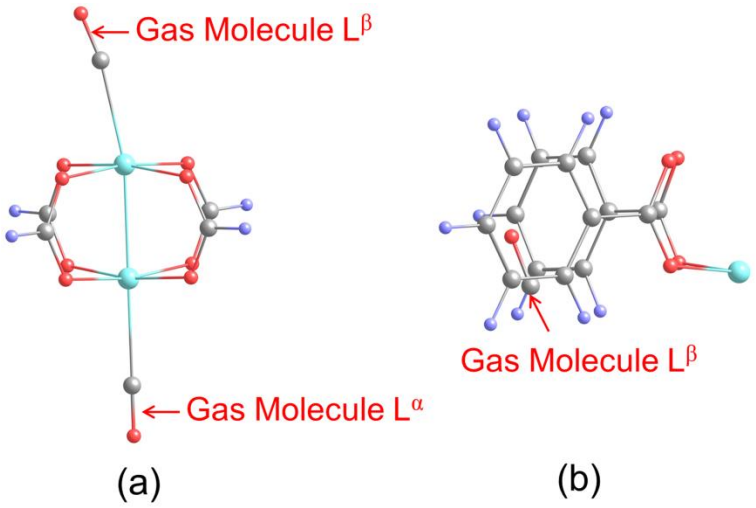

Figure S2. Small models (a) SM1 and (b) SM2 employed for high-level calculations in the ONIOM method.

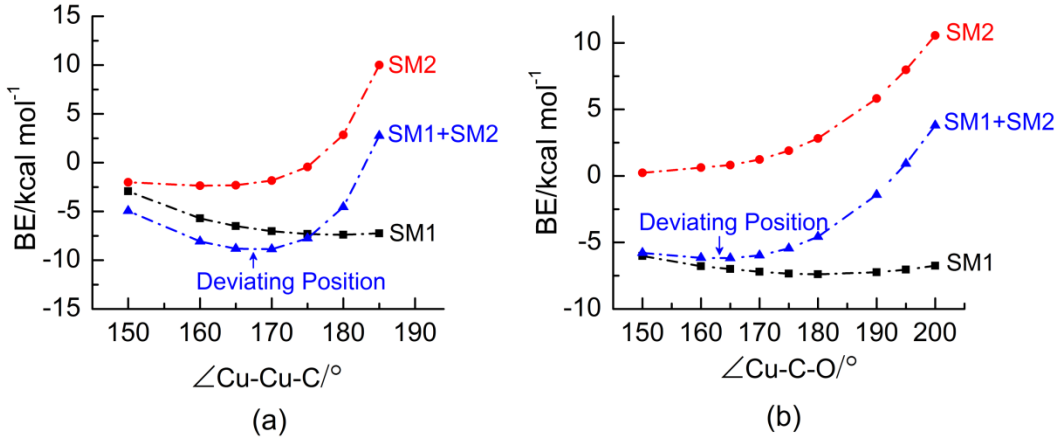

Figure S3. ωB97XD-calculated potential energy surfaces for CO interactions with (a) SM1 and (b) SM2 models.

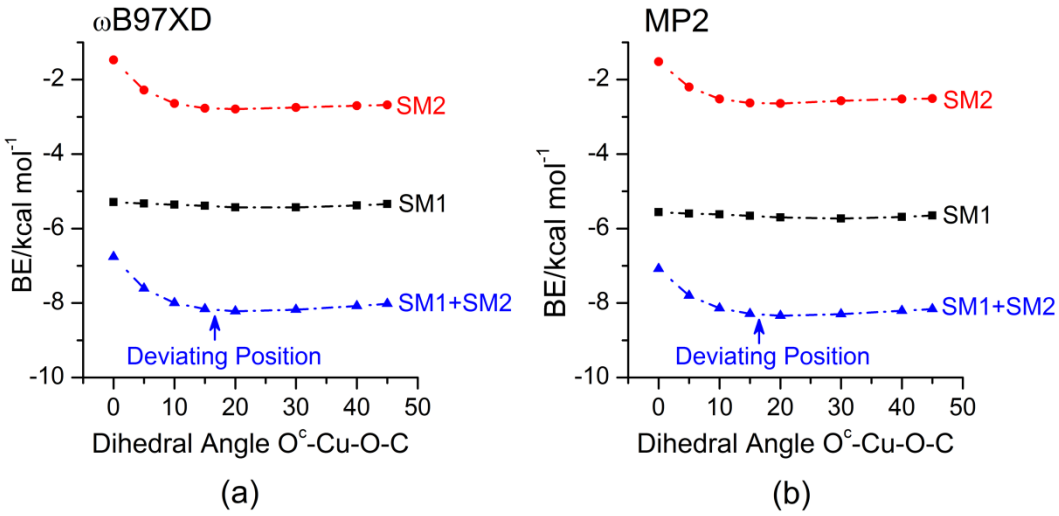

Figure S4. (a) ωB97XD- and (b) MP2-calculated potential energy surfaces for CO_2 interactions with SM1 and SM2.

REFERENCES

(1) Sato, H.; Kosaka, W.; Matsuda, R.; Hori, A.; Hijikata, Y.; Belosludov, R. V.; Sakaki, S.; Takata, M.; Kitagawa, S. Self-Accelerating CO Sorption in a Soft Nanoporous Crystal. *Science* **2014**, *343*, 167-170.